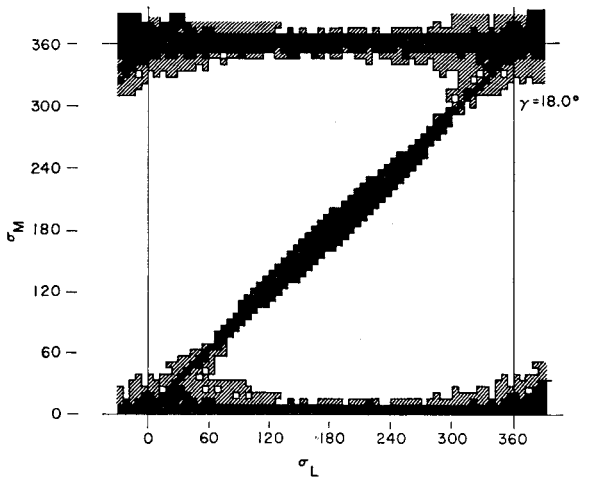

Fig. 5. A map of the σ_L, σ_M plane for $\gamma = 18.0°$.

White: physically realizable ring circulators;
Black: no ring circulator exists;
Shaded: borderline cases, uncertain due to rounding-off errors.

overall transmission coefficient E_2, (9). Finally, the parameter of merit M is evaluated.

A map illustrating the range of soluble cases is shown in Fig. 5. The particular range of cases shown there is for the value $\gamma = 18.0°$ and $\sigma_c = 0$, with σ_a and σ_b ranging from 0° to 360° (σ_L and σ_M are the same as σ_a and σ_b, respectively). The white areas represent physically realizable cases; the black, inadmissible cases. The diagonally shaded regions are borderline cases which are ambiguous because of rounding-off errors in the computation. A series of eleven such maps, for $\gamma = 0°$, 4.5°, · · ·, 45.0°, show that well over half of the "parameter space," whose coordinates are σ_a, σ_b, σ_c, γ, is occupied by physically realizable cases.

Acknowledgment

The support and encouragement of D. H. Temme and other members of the group is hereby acknowledged. I also wish to acknowledge the invaluable assistance of J. Tabasky and C. Work of the Computer Facility of the Lincoln Laboratory.

References

[1] Auld, B. A., The synthesis of symmetrical waveguide circulators, *IRE Trans. on Microwave Theory and Techniques*, vol MTT-7, Apr 1959, pp 238–246.
[2] Bosma, H., On the principle of stripline circulation, *Proc. IEE* (London), vol 109B, suppl 21, 1962, p 137.
——, On stripline *Y*-circulation at UHF, *IEEE Trans. on Microwave Theory and Techniques*, vol MTT-12, Jan 1964, pp 61–72.
[3] Grace, M., and F. R. Arams, Three-port ring circulators, *Proc. IRE (Correspondence)*, vol 48, Aug 1960, p 1497.
[4] Vartanian, P. N., The theory and applications of ferrites at microwave frequencies, Sylvania EDL Rept. DDC-101, 888, Sylvania Defense Lab., Mountain View, Calif., Apr 1956.
[5] Montgomery, C. G., R. H. Dicke, and E. M. Purcell, *Principles of Microwave Circuits*, M.I.T. Rad. Lab. Ser., vol 8, ch. 12, New York: McGraw-Hill, 1948.

A 7-Gc/s Narrow-Band Waveguide Switch Using *p-i-n* Junction Diodes

H. J. PEPPIATT, MEMBER, IEEE, A. V. McDANIEL, JR., AND J. B. LINKER, JR., SENIOR MEMBER, IEEE

***Abstract*—A narrow-band waveguide switch with power capability in excess of 8 watts has been designed in WR137 waveguide. *p-i-n* diodes are used in band elimination filter sections. The attenuation in the reject band is greater than 80 dB over a 10 Mc/s range, and the passband loss is less than 0.5 dB.**

Introduction

IN BOTH the forward and reverse bias conditions, the *p-i-n* diode approximates very closely a linear circuit element. Hence, conventional circuit analysis and synthesis can be used in the design of components using these diodes. The microwave switch, to be described here, can be designed by the use of waveguide band elimination filter synthesis.

Manuscript received June 15, 1964; revised October 19, 1964.
The authors are with the Communication Products Dept., General Electric Co., Lynchburg, Va.

Band Elimination Synthesis

For completeness, a very brief resume of a band elimination synthesis is included. The low-pass prototype of Fig. 1 can be synthesized to a given response by modern network techniques. Extensive tables giving the element values for a wide variety of responses are available.[1] The frequency and impedance transformations necessary to arrive at a quarter-wave coupled band elimination filter are shown in Fig. 1. It is easily shown that

$$y_p'' = -jY_0 g_p \frac{\omega_b}{\omega_0 \Omega} \tag{1}$$

[1] Weinberg, L., *Network Analysis and Synthesis*, New York: McGraw-Hill 1962, pp 604–631.

where ω_b is the bandwidth of the filter, ω_0 is the band elimination center frequency, and $\Omega=(\omega/\omega_0-\omega_0/\omega)$. From a practical point of view, it is convenient to represent each element in Fig. 1(c) by its doubly loaded[2] Q (this procedure is similar to that of Mumford[3] for band-pass quarter-wave coupled filters). From this, one obtains

$$Q_p = \frac{2Q_T}{g_p} \tag{2}$$

where $Q_T=\omega_0/\omega_b$, the loaded Q of the filter, and Q_p is the required doubly loaded Q of each section.

The effect of incidental dissipation at ω_0 can be predicted by the following relations:

$$L_r(\omega_0) = \left|\frac{1}{\Gamma(\omega_0)}\right|^2 \simeq \left|\frac{g_1\frac{Q_u}{Q_T}-1}{g_1\frac{Q_u}{Q_T}+1}\right|^2 \tag{3}$$

$$L_d(\omega_0) \simeq \left(\frac{Q_u}{Q_T}\right)^{2n}\cdot\left(\frac{g_1g_2\cdots g_n}{2}\right)^2 \tag{4}$$

where $\Gamma(\omega_0)$ is the reflection coefficient at ω_0, $L_r(\omega_0)$ is the loss encountered upon reflection at band center, $L_d(\omega_0)$ is the insertion loss (or attenuation) at band center, and Q_u is the unloaded Q of each tuned circuit (cavity). These equations are derived easily by noting the $ABCD$ matrix at ω_0 of the circuit of Fig. 1(b). They can also be derived from more general equations of Young et al.[2]

A waveguide realization of a single-section band elimination filter[4] is shown in Fig. 2 along with the equivalent circuit.[5] The loaded $Q(Q_p)$ can be measured as a function of the coupling hole geometry. For resonance at ω_0, the length l_s of the stub transmission line is

$$l_s = \frac{1}{\beta_{g0}}\tan^{-1}\frac{1}{B_b} \tag{5}$$

where β_{g0} is the guide phase constant at ω_0, and B_b is the coupling susceptance (see Fig. 2). The admittance of B_b and the stub line is y where

$$y = jB_b - j\cot\left[\frac{1}{A}\arctan\left(\frac{1}{B_b}\right)\right] \tag{6}$$

and

$$A = \frac{\omega_0^2-\omega_c^2}{\omega^2-\omega_c^2}$$

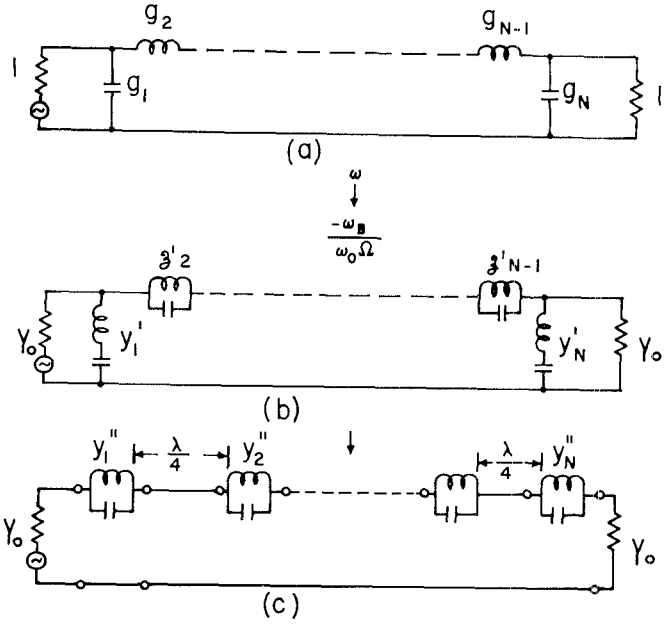

Fig. 1. Transformation from lowpass prototype to band elimination filter.

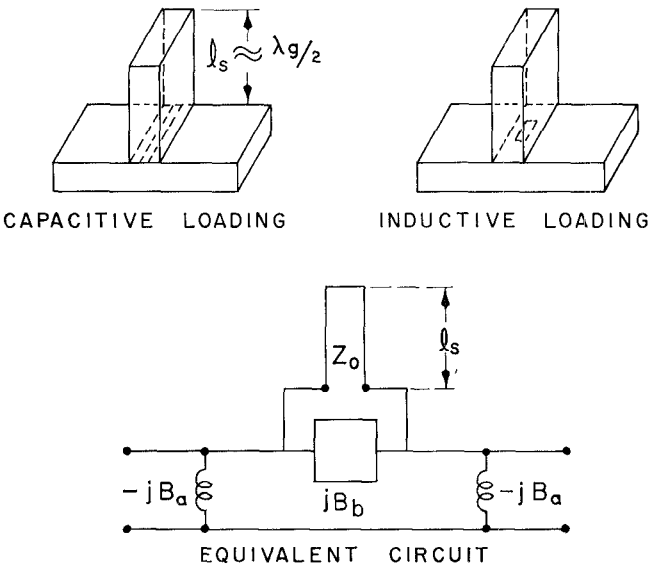

Fig. 2. Waveguide band elimination filter section.

where ω_c is the cutoff frequency of the guide. The length l between sections of a multisection filter is given by

$$l = \frac{1}{\beta_{g0}}\arctan\left(\frac{1}{B_a}\right) \tag{7}$$

and because of the small values of B_a[5] these lengths are extremely close to an odd multiple of $\lambda_g/4$.

Normal filter synthesis thus requires only knowledge of the type of filter desired, the center frequency, and the specified bandwidth. Requisite values of Q_p can be determined from the value of Q_T and the g_p's. Also readily found are the line lengths l_s and l. Filter specifications may be chosen by taking into consideration acceptable values of reflection loss and insertion loss.

[2] Young, L., et al., Microwave band-stop filters with narrow stop bands, *IRE Trans. on Microwave Theory and Techniques*, vol MTT-10, Nov 1962, pp 416–427. (An alternate approach using the "reactance slope parameter" is offered in this reference.)

[3] Mumford, W. W., Maximally flat filters in waveguide, *Bell Sys. Tech. J.*, vol 27, Oct 1948, pp 684–713.

[4] Southworth, G. C., *Principles and Applications of Waveguide Transmission*, Princeton N. J.: Van Nostrand 1950, p 305.

[5] Marcuvitz, N., *Waveguide Handbook, Rad. Lab. Ser.*, vol 10. New York: McGraw-Hill, 1951, pp 351–363.

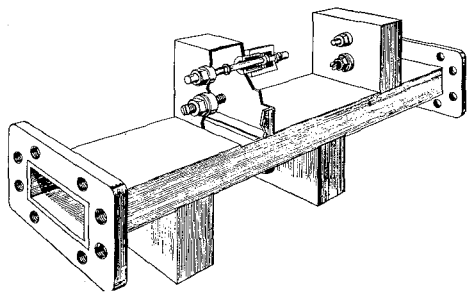

Fig. 3. Waveguide switch using *p-i-n* junction diodes.

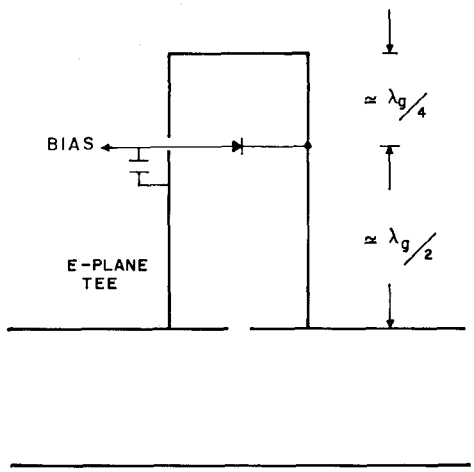

Fig. 4. Schematic of single element switch.

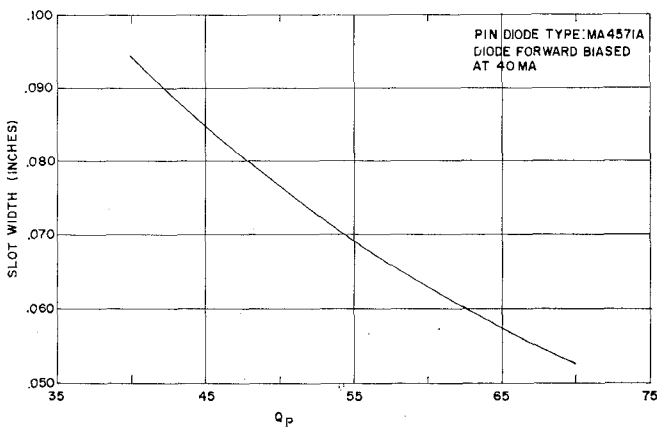

Fig. 5. Loaded Q vs. capacitive coupling slot width.

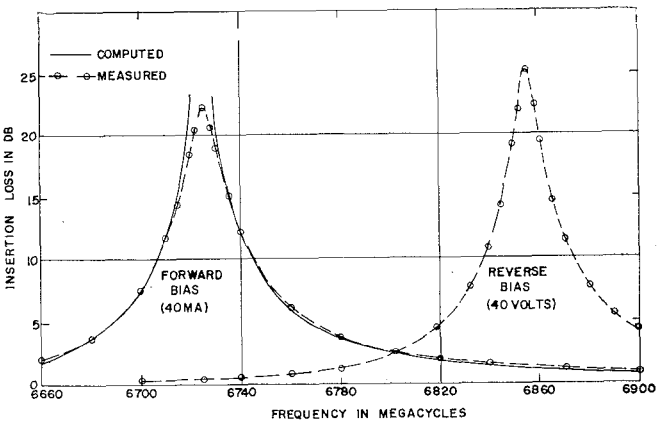

Fig. 6. Characteristics of single cavity filter switch.

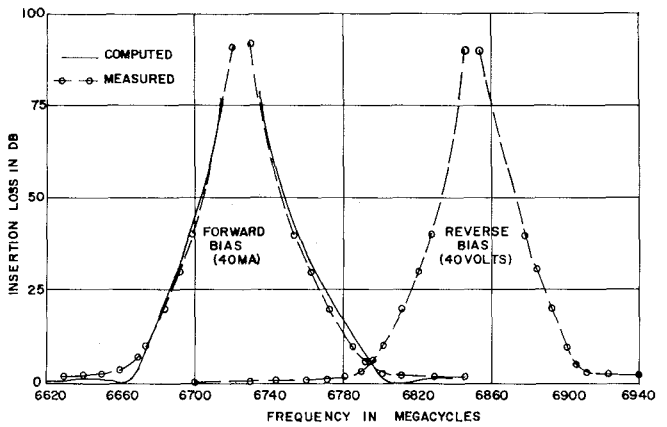

Fig. 7. Characteristics of four cavity filter switch.

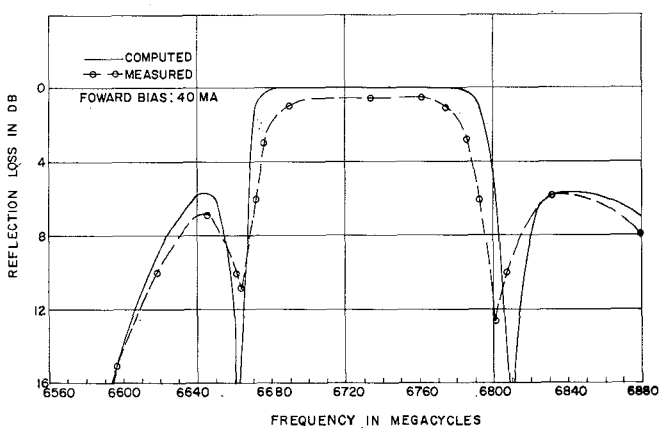

Fig. 8. Reflection loss of four cavity filter switch.

Switch Design

A switch can be realized by using a band stop filter with a semiconductor junction diode placed in each resonator to provide a means of changing its resonant frequency with diode bias. Figure 3 shows such a filter (four-section) with its diodes. The diode mount choke section, and cavity tuning screw are shown in the cutaway view. Capacitive coupling slots are used. The spacing between cavities is $3\lambda_g/4$ rather than $\lambda_g/4$ to avoid excessive direct coupling. The approximate location of the diode in each cavity is indicated schematically in Fig. 4. If a filter section is tuned with the diode forward biased, the resonant frequency shifts to a higher frequency when the bias is reversed. Such a diode must have two impedance states: one approaching an open circuit (reverse bias), and the other a short circuit (forward bias). The series resistance in the forward bias state must be small so that diode temperature rise and insertion loss will be small. The capacitance of the diode must be small in the reverse bias state so that adequate filter detuning (and thus switching) is achieved with bias change. The *p-i-n* type diode satisfies these require-

ments.[6] Also, it has a rather high Q which offers advantages of lower loss and narrow-band design as desired.

A plot of Q_p (loaded Q) vs. capacitive coupling slot size is given in Fig. 5. This represents measured data taken on a single-section filter.

Figure 6 shows the measured and computed (lossless case) insertion loss of a single-section filter vs. frequency for both states of the switch. From the measured insertion loss at band center and (2), the unloaded Q_u can be estimated. These measurements should be made for both the forward and the reverse bias conditions. With this data, it is possible to design and meet many different switching specifications.

[6] Hunton, J. K., and A. G. Ryals, Microwave variable attenuators and modulators using PIN diodes, *IRE Trans. on Microwave Theory and Techniques*, vol MTT-10, Jul 1962, pp 262–273.

Figure 7 shows the attenuation characteristics of a four-section equal Q filter switch for both conditions of switching while Fig. 8 shows the reflection loss. It is to be noted that the attenuation is in excess of 80 dB for a bandwidth of 10 Mc/s in the reject band, and that the insertion loss in the pass band at a frequency displacement of 120 Mc/s is less than 0.5 dB. Measurements of switching time show it to be less than 1 μs.

When the characteristics of this switch operating under 8 watts of RF power were checked over a temperature range of plus 65°C to minus 10°C, there was no change measured in response or loss attributable to the diodes.

Acknowledgments

The authors acknowledge the contributions of R. E. Neidert relative to switch evaluation under conditions of high power and changing temperature.

A High-Power Ferroelectric Limiter

M. COHN, SENIOR MEMBER, IEEE, AND A. F. EIKENBERG

Abstract—**Ferroelectric limiters capable of handling peak input power levels in excess of 25 kW with a small signal insertion loss of 0.5 dB have been built. The measured performance and a theoretical analysis have shown that excellent limiting characteristics can be obtained, and that saturation power output levels ranging from a few watts up to megawatts can be obtained with ferroelectric pellets that can be conveniently fabricated. The limited available material data indicates that ferroelectric limiters will offer their greatest advantage in the HF, VHF, and UHF bands. The theoretical analysis of the expected temperature rise within the ferroelectric pellet has shown that, by proper design, very-high-average power levels also can be handled. A recovery time of less than ten microseconds has been measured.**

Introduction

A NEW TYPE of solid state high-power limiter, which utilizes the large signal nonlinear characteristics of ferroelectric materials, has been developed. Since the nonlinear action takes place within a bulk ceramic material, the high-power handling capability was expected. However, a deterrent to the use of ferroelectric materials in devices such as high-power limiters is the lack of sufficient data on the electrical properties of these materials. This is particularly true in the case of their large signal properties, knowledge of which is essential in order to design and predict the performance of limiters.

Manuscript received July 29, 1964; revised October 19, 1964. The research for this work was sponsored by the Navy Department, Bureau of Ships, Electronics Division under Contract NObsr-87394.

The authors are with the Advanced Technology Corporation (formerly the Research Division of Electronic Communications, Inc.), Timonium, Md.

Properties of the Ferroelectric Material

The ferroelectric material used was a ceramic mixture of 45 per cent lead titante and 55 per cent strontium titanate. This mixture is referred to in mole per cent. Its small signal electrical properties were determined from measurements made on a small circular parallel-plate capacitor. This small ferroelectric capacitor (diameter = 0.033 inch, height = 0.050 inch) was located between the end of the center conductor and an end plate of a special coaxial holder. A diagram of the measurement system is shown in Fig. 1. A heating coil was placed around that portion of the coaxial holder containing the ferroelectric capacitor. A thermocouple was used to monitor temperature. Direct current voltage, up to 2000 volts, could be applied across the plates of the ferroelectric capacitor.

The small signal dielectric constant (K) and dielectric loss tangent of the 45 per cent $PbTiO_3$–55 per cent $SrTiO_3$ ceramic material were measured as a function of temperature (T) at a frequency of 218 Mc/s. The dielectric constant values were determined from standard input impedance measurements made with a slotted line. The loss tangent was measured using a cavity